Modeling of the Wind Turbine With a Doubly Fed Induction Generator for Grid Integration Studies

Yazhou Lei, Alan Mullane, Gordon Lightbody, and Robert Yacamini

***Abstract*—Due to its many advantages such as the improved power quality, high energy efficiency and controllability, etc. the variable speed wind turbine using a doubly fed induction generator (DFIG) is becoming a popular concept and thus the modeling of the DFIG based wind turbine becomes an interesting research topic. Fundamental frequency models have been presented but these models are often complex with significant numerical overhead as the power converter block consisting of power control, rotor side and grid side converter control and DC link are often simulated in detail. This paper develops a simple DFIG wind turbine model in which the power converter is simulated as a controlled voltage source, regulating the rotor current to meet the command of real and reactive power production. This model has the form of traditional generator model and hence is easy to integrate into the power system simulation tool such as PSS/E. As an example, the interaction between the Arklow Bank Wind Farm and the Irish National Grid was simulated using the proposed model. The model performance and accuracy was also compared with the detailed model developed by DIgSILENT. Considering the simplification adopted for the model development, the limitation and applicability of the model were also discussed in this paper.**

***Index Terms*—Induction generators, power system transient stability, reactive power control, variable speed drives, wind power generation.**

NOMENCLATURE

β	Wind turbine blade pitch angle.
C_f	Wind turbine blade design constant.
C_p	Wind turbine power coefficient.
E'	Voltage behind the transient impedance.
H_r, H_m	Generator rotor and wind turbine shaft inertia.
i	Current.
K_P, K_I	Coefficients for the proportional-integral controller.
K_s	Shaft stiffness coefficient.
λ	Wind turbine tip-speed ratio.
L	Inductance,
ω_s, Ω_m, Ω_r	Synchronous, wind turbine shaft, and generator rotor angle speed.
ψ	Flux linkage.
P, Q	Active and reactive power.
ρ	Air density.
r	Resistance.
R	Wind turbine blade radius.
s	Rotor slip.
θ_s, θ_m, θ_r	Terminal voltage, wind turbine shaft and generator rotor angle position.
T_0'	Rotor circuit time constant.
T_{em}	Electromagnetic torque.
T_m	Mechanical torque act on the generator rotor.
T_r	Low-pass time constant for rotor voltage control.
T_w	Wind turbine prime torque from wind.
v	Voltage.
V_w	Wind speed.
X, X', X_m	Steady-state, transient, and magnetizing reactance.
	Symbols
$1/s$	Integral operator.
Δ	Deviation from normal value.
MPT	Maximum power tracking logic.
	Suffices, Superscripts
d, q	Direct and quadrature axis components.
max, min	Maximum and minimum value.
s, r	Generator's stator and rotor components.
x, y	Horizontal and vertical components in the common reference frame.
$*$	Reference value.
$'$	Transient state component.

Manuscript received November 19, 2003; revised April 15, 2004. This work was supported by Enterprise Ireland and ESB Ireland. Paper no. TEC-00343-2003.

The authors are with the Department of Electrical and Electronic Engineering, University College Cork, Cork, Ireland (e-mail: leiyazhou@yahoo.com).

Digital Object Identifier 10.1109/TEC.2005.847958

I. INTRODUCTION

WITH growing concerns about environmental pollution and a possible energy shortage, great efforts have been taken by the governments around the world to implement renewable energy programs, based mainly on wind power, solar energy, small hydro-electric power, etc. Ever since the first large grid connected wind farm appeared in California (U.S.) in the 1980s, wind power generation has been undergoing a significant development. With improving techniques, reducing costs and low environmental impact, wind energy seems certain to play a major part in the world's energy future. As the wind power penetration continually increases, power utilities concerns are shifting focus from the power quality issue to the stability problem caused by the wind power connection [1]–[3]. In such cases, it becomes important to consider the wind power impact properly in the power system planning and operation. Unfortunately, few power system analysis tools have included wind turbine models such as have been developed for traditional power generators. Therefore, when carrying out wind power embedded network planning or operation analysis, engineers have to put much effort into the modeling of the wind turbines rather than concentrating on the problem itself. Hence, a wind turbine model compatible with commercial power system analysis tools, like PSS/E, is in imminent need.

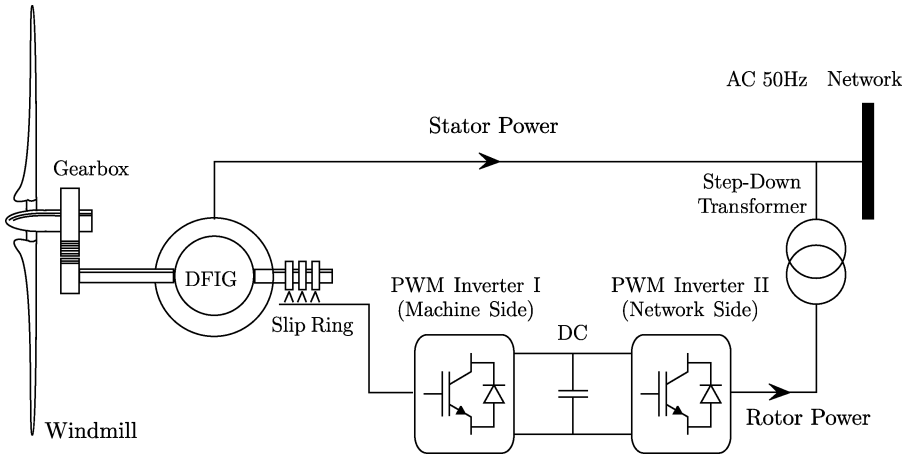

Fig. 1. Scheme of a DFIG equipped wind turbine.

In the early stage of wind power development, most wind farms were equipped with fixed-speed wind turbines and induction generators. Since such wind generators can only operate at a constant speed, the power efficiency is fairly low for most wind speeds. To improve their efficiency, many modern wind generators adopt a variable speed operation in one of two ways: direct ac to ac frequency converters, such as the cycloconverters [4], [5]; or using voltage controlled inverters (ac-dc-ac), which convert power at varying frequencies at the variable-speed generator to dc, and then use some form of power electronics to convert the dc power back to ac at a fixed frequency appropriate for the grid connection [6], [7].

Amongst many variable speed concepts, the DFIG equipped wind turbine has many advantages over others [6]. For example, the power converter in such wind turbines only deals with rotor power, therefore the converter rating can be kept fairly low, approximately 20% of the total machine power. This configuration allows for variable speed operation while remaining more economical than a series configuration with a fully rated converter. Other features such as the controllability of reactive power help DFIG equipped wind turbines play a similar role to that of synchronous generators.

Whilst the simulation of the DFIG wind turbine has been dealt with in many publications [7]–[13], most of them were electromagnetic models suitable for the detailed study of the power converter and its control strategy. To meet the demand of power system simulation, the fundamental frequency DFIG wind turbine model was also proposed in [2], [14], and [15]. The power converter model in these papers was still complex, consisting of the power controller, rotor side and grid side converter controller and dc link. However, for power system analysis, the internal dynamics of power converter are not of interest. As a small simulation time step is required by the current controller, such models are time consuming and inappropriate with traditional power system simulation tools such as PSS/E. This paper proposes a simplified model, representing the DFIG in terms of a voltage behind the transient reactance. Assuming an ideal power converter, a voltage source controlling the rotor current is applied to the rotor circuit to simulate the effect of the power converter. In addition, the blade pitch control and a soft coupling shaft system were also modeled to an appropriate extent. Section II discusses the DFIG transient model and Section III presents the control scheme and protection scheme model. In Section IV, the proposed model was applied to analyze the interaction between the Arklow Bank Wind Farm and the Irish National Grid. The model limitation and applicability were also discussed by comparison with the fundamental frequency model presented by DIgSILENT.

II. Transient Model of a DFIG

A typical scheme of a DFIG equipped wind turbine is shown in Fig. 1. Two voltage fed PWM converters are inserted back-to-back in the rotor circuit, which connect the slip ring terminals to the ac supply network. By adjustment of the switching of the Insulated Gate Bipolar Transistors in both converters, the power flow between the rotor circuit and the supply can be controlled both in magnitude and in direction [8], [9], [13]. This is effectively the same as connecting a controllable voltage source to the rotor circuit [16]. The DFIG can be regarded as a traditional induction generator with a nonzero rotor voltage. With the stator transients neglected, the per unit electrical equations of the DFIG can be written in phasor form as follows [16], [17].

Stator voltage

$$v_{ds} = r_s i_{ds} + \omega_s \psi_{qs} \tag{1}$$

$$v_{qs} = r_s i_{qs} - \omega_s \psi_{ds}. \tag{2}$$

Rotor voltage

$$v_{dr} = r_r i_{dr} - s\omega_s \psi_{qr} + \frac{d\psi_{dr}}{dt} \tag{3}$$

$$v_{qr} = r_r i_{qr} + s\omega_s \psi_{dr} + \frac{d\psi_{qr}}{dt}. \tag{4}$$

Flux linkage

$$\psi_{ds} = -L_{ss} i_{ds} + L_m i_{dr} \tag{5}$$

$$\psi_{qs} = -L_{ss} i_{qs} + L_m i_{qr} \tag{6}$$

$$\psi_{dr} = -L_m i_{ds} + L_{rr} i_{dr} \tag{7}$$

$$\psi_{qr} = -L_m i_{qs} + L_{rr} i_{qr}. \tag{8}$$

Electromagnetic torque

$$T_{em} = \psi_{qr} i_{dr} - \psi_{dr} i_{qr}. \tag{9}$$

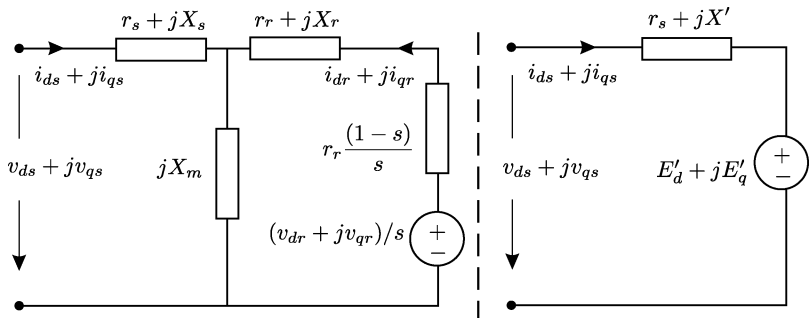

Fig. 2. Steady-state and dynamic equivalent circuits of a DFIG.

In the case of the traditional induction machine, the rotor voltage in (3) and (4) are zero. To reduce (1) to (8) to a form suitable for implementation in a transient stability program, it is necessary to eliminate the rotor currents and rewrite the equations in terms of a voltage behind a transient reactance. Thus, by solving (1), (6), and (8), we get

$$v_{ds} = r_s i_{ds} - X' i_{qs} + E'_d. \tag{10}$$

Similarly, we can also get

$$v_{qs} = r_s i_{qs} + X' i_{ds} + E'_q \tag{11}$$

where

$$E'_d = \frac{\omega_s L_m \varphi_{qr}}{L_{rr}} \tag{12}$$

$$E'_q = \frac{-\omega_s L_m \varphi_{dr}}{L_{rr}} \tag{13}$$

$$X' = \omega_s \left(\frac{L_{ss} - L_m^2}{L_{rr}} \right). \tag{14}$$

By eliminating the rotor currents in (3) and (4), and expressing the rotor flux linkage in terms of E'_d, E'_q, the following equations describing the rotor circuit dynamics can be obtained:

$$\frac{dE'_d}{dt} = s\omega_s E'_q + \omega_s v'_{qr} - \frac{1}{T'_0}\left[E'_d + (X - X')i_{qs}\right] \tag{15}$$

$$\frac{dE'_q}{dt} = -s\omega_s E'_d - \omega_s v'_{dr} - \frac{1}{T'_0}\left[E'_q - (X - X')i_{ds}\right] \tag{16}$$

where

$$v'_{dr} = \frac{v_{dr} X_m}{(X_m + X_r)} \tag{17}$$

$$v'_{qr} = \frac{v_{qr} X_m}{(X_m + X_r).} \tag{18}$$

Fig. 2 show the steady-state and dynamic equivalent circuit of the DFIG, respectively.

By eliminating the rotor currents i_{dr}, i_{qr} in the electromagnetic torque (9), and when $\omega_s = 1.0$ pu, we find

$$T_{em} = E'_d i_{ds} + E'_q i_{qs}. \tag{19}$$

By substituting (10) and (11), the per unit electromagnetic torque can be written as

$$T_{em} = v_{ds} i_{ds} + v_{qs} i_{qs} - r_s \left(i_{ds}^2 + i_{qs}^2\right). \tag{20}$$

Generally, the power losses associated with the stator resistance are small enough to be ignored, hence the approximation of electromagnetic power or torque can be written as

$$T_{em} = P_s = v_{ds} i_{ds} + v_{qs} i_{qs} \tag{21}$$

while the reactive power that the stator absorbs from, or injects into the power system can be calculated as

$$Q_s = v_{qs} i_{ds} - v_{ds} i_{qs}. \tag{22}$$

Accordingly, the rotor motion of the DFIG can be written as

$$2H_r \frac{d\Delta\Omega_r}{dt} = -T_{em} - T_m. \tag{23}$$

For the case of generators, the value of T_{em} corresponding to the direction of current and voltage shown in Fig. 2 is negative.

Similarly, the rotor power (also called slip power) can be calculated as

$$P_r = v_{dr} i_{dr} + v_{qr} i_{qr} \tag{24}$$

$$Q_r = v_{qr} i_{dr} - v_{dr} i_{qr}. \tag{25}$$

When the power losses in the converters are neglected, the total real power P_e injected into the main network equals to the sum of the stator power P_s and the rotor power P_r. The reactive power Q_e exchanged with the grid equals to the sum of stator reactive power Q_s and that of grid side converter Q_g. In this paper, the value of Q_g was fixed to simplify the model.

Additionally, since the wind turbine shaft and generator rotor are coupled together via a gearbox, the wind turbine shaft system should not be considered stiff. The interaction between the windmill and rotor makes the shaft motion more complex than the lumped-mass system. To account for this effect properly, an additional equation has been adopted to describe the motion of the windmill shaft [2]

$$2H_m \frac{d\Delta\Omega_m}{dt} = T_m - T_w \tag{26}$$

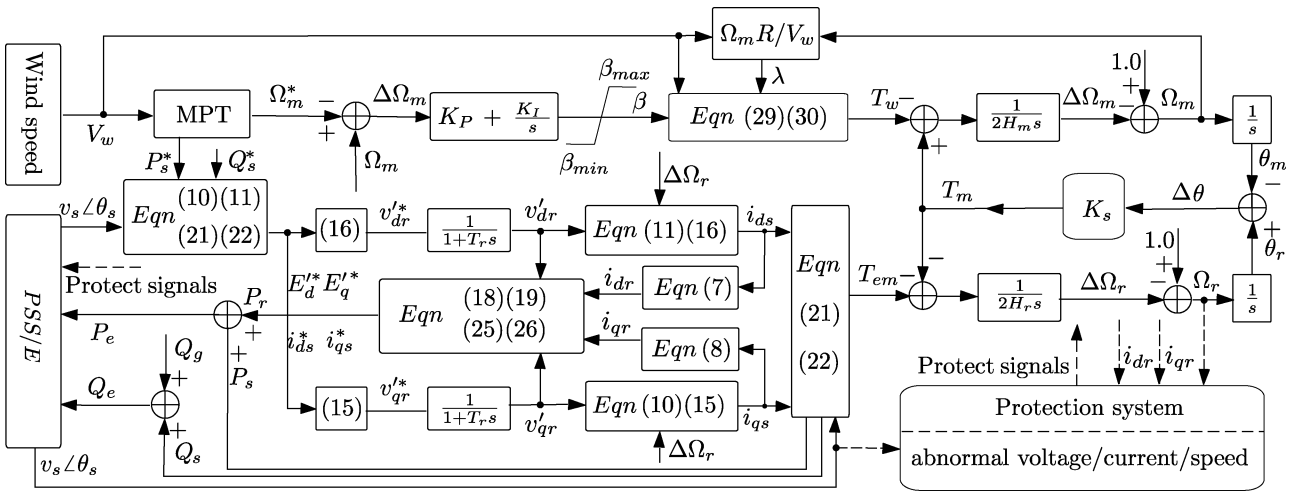

Fig. 3. Simulation scheme for a doubly-fed induction generator equipped wind turbine and interface with PSS/E.

where the mechanical torque T_m can be represented by the twist angle between the wind turbine shaft and the generator rotor

$$T_m = K_s(\theta_r - \theta_m). \tag{27}$$

III. Control Scheme Description

The DFIG wind turbine control usually consists of two parts: the mechanical control on the wind turbine blade pitch angle and the electrical control on the power converter. The power converter usually includes the power control, the rotor side current control, dc link dynamics, the grid side current control and the PWM scheme [2], [14], [15]. In this paper, a controllable voltage source in the rotor circuit, as shown in Fig. 2 was used to simulate the power converter. Such simplifications allows for reduction of the model order whilst retaining the capability of observing principle features of the converter such as the maximum current levels. Such capability is important for assessing criteria such as fault-ride-through performance.

In power system analysis programs, the state variables for generator models are usually referred to a common stationary X-Y axis frame. The angular position of the DFIG terminal voltage in this reference frame can be determined as

$$\theta_s = \tan^{-1}\frac{v_y}{v_x}. \tag{28}$$

Upon aligning the direct axis of the reference frame with the stator voltage position given by (28), v_{qs} becomes zero, and v_{ds} is then equal to the amplitude of terminal voltage. Thus according to (21) and (22), the real and reactive power are proportional to i_{ds} and i_{qs} respectively. This is the basis of independent control of torque and reactive power in the DFIG. According to (5) and (6), the stator currents i_{ds} and i_{qs} are related to the rotor currents i_{dr} and i_{qr} respectively. By adjusting rotor voltage appropriately, the desired rotor currents, and hence the desired stator currents corresponding to the optimal electromagnetic torque and the desired Var flow/power factor can be achieved. As the bandwidth of the voltage source converter, under PWM control, is very large compared with the pitch control or the shaft motion, the rotor voltage is calculated algebraically in the simulation. A time delay T_r is included in the rotor voltage control in Fig. 3 to account for the delays associated with the measurement and voltage vector computation for a voltage source converter.

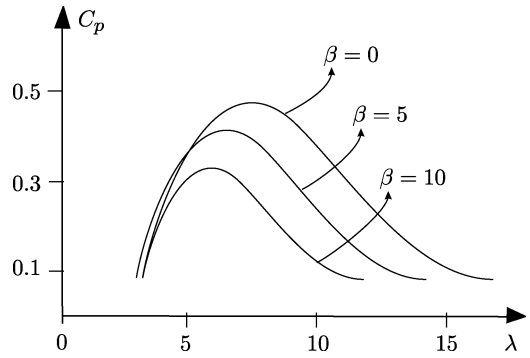

Fig. 4. Power efficiency curves versus tip-speed ratio.

To work effectively, the power converter must be controlled in collaboration with the wind turbine pitch control. As has been discussed in many published papers, the efficiency C_p is a function of the tip speed ratio λ and the pitch angle β (in degrees). Here λ is the ratio between the linear speed of the blade tip with respect to the incoming wind speed, $\lambda = \Omega_m R/V_w$. As can be seen from Fig. 4, the value of C_p can only approach its maximum point at some optimal λ. In other words, given a particular wind speed, there is a unique rotational speed required to achieve the goal of Maximum Power Tracking (MPT). At below the rated wind speed, the wind turbine operates in the variable speed mode, and the rotational speed is adjusted such that the maximum value of C_p is achieved. With increasing wind speed, the rotational speed of wind turbine increases. Once the rotor speed exceeds its upper limit, the pitch controller will begin to increase the pitch angle to shed some of the aerodynamic power. As the pitch angle increases, the value of C_p decreases. The relationship between C_p, λ and pitch angle β can be approximated by [18]

$$C_p = \frac{1}{2}\left(\frac{RC_f}{\lambda} - 0.022\beta - 2\right)e^{-0.255\frac{RC_f}{\lambda}} \tag{29}$$

where C_f is a blade design constant. When the wind speed is V_w, the wind torque can be calculated as

$$T_w = \frac{0.5\rho\pi R^2 C_p V_w^3}{\Omega_m}. \tag{30}$$

The pitch controller is designed within the working limits of the pitch actuator, and hence it cannot change the pitch angle too fast or beyond the limits [19]. This control scheme is also shown in Fig. 3, in combination with the rotor control system. According to (21), (23), the desired wind turbine stator power P_s^* can be calculated based on the value of T_m^*, determined by the Maximum Power Tracking logic. The value of Q_s^* depends on the chosen reactive power control strategy, i.e., fixed Var flow or fixed power factor.

Apart from the wind turbine, DFIG and relevant controller models mentioned above, three protective functions namely; abnormal voltage, current and speed protection were also implemented in the proposed model. The under/over-voltage unit monitors the voltage at the high voltage side of the transformer. If the voltage falls and remains below, for example, to about 0.9 pu, the machine will be disconnected within a minute or two to protect the power converters. If the supply voltage falls to an even lower value, they will be cut off instantaneously [20]. The under/over-speed unit monitors the rotor speed and triggers the machine in emergency; the over-current protection, also called Crow-Bar protection in the DFIG, protects the rotor side converter against over currents. When the rotor current exceeds a threshold value, the converter is blocked and bypassed through an additional impedance to avoid the disconnection of the wind generator [15]. The complete simulation scheme for a DFIG equipped variable speed wind turbine is shown in Fig. 3. It should be noted that only the main inputs into some blocks were indicated on the diagram. Other input variables that can be easily found in the equations are not given to keep the diagram clear.

IV. Simulation Using PSS/E

In the following simulation, a simplified model of the Irish National Grid (ING) and of the planned Arklow Bank offshore wind park were used to test the performance of the model described above. The ING is an isolated power system with the capacity of 4500 MW, whose backbone is a 220-kV looped network connected with two un-looped 400-kV transmission lines, which will consume the total power output from the wind park when commissioned. The example used in this paper was confined to the phase-one project of the wind park, which consists of seven GE3.6 MW wind turbines (see Table I). A 10-km submarine cable which connects the wind park to the 38-kV distribution network was included in the model. A total capacity 80 Mvar of switched inductors was also included to absorb the excessive reactive power generated by the cable (Table II). The response of the wind turbine to a step increase in the wind speed and to an electrical bus fault were studied. As no small time constants were included in the proposed wind turbine model, the simulation was carried out in PSS/E using the normal half cycle step size.

TABLE I
Wind Turbine Parameters

Para.	Value	Units	Para.	Value	Units
P_{rated}	3.6	MW	Ω_{max}	15.3	rpm
Ω_{rated}	14.0	rpm	Ω_{min}	8.5	rpm
r_s	.00779	p.u.	K_P	75.0	deg.
L_s	.07937	p.u.	K_I	25.0	deg./s
r_r	.025	p.u.	θ_{max}	27.0	deg.
L_r	.40	p.u.	θ_{min}	.0	deg.
L_m	4.1039	p.u.	$\lvert\frac{d\theta_{max}}{dt}\rvert$	10.0	deg./s
H_r	.5	s	T_r	.05	s
H_m	2.5	s	C_f	.733	p.u.
K_s	.35	p.u./rad.	R	50.0	m

TABLE II
Test System Parameters

Parameter	Value	Unit
Wind farm compensation reactor	80.0	Mvar
submarine cable impedance	j.006	p.u.
submarine cable capacitance	.45	p.u.

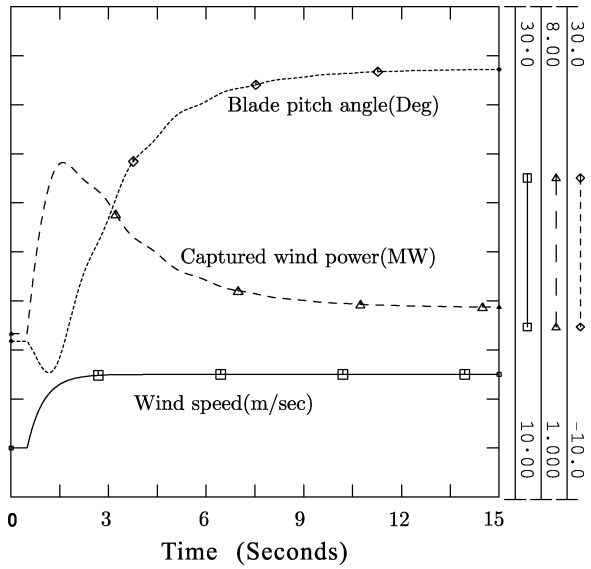

Fig. 5. Wind turbine pitch angle and captured power versus wind speed.

In the first case, the initial wind speed was assumed to be 12 m/s, and was then ramped to the rated value of 15 m/s in about 1.5 s. To consider wake effects in wind speeds due to the spacial siting of wind turbines, the wind change was assumed to act on the wind turbines one by one with an interval of 0.5 s. As can be seen from Fig. 5, the captured wind power increased in response to the incoming wind speed. Once the power exceeded the rated value, the pitch control system began to regulate the pitch angle. As the pitch angle increased, the power efficiency of the wind turbine decreased to reduce wind energy capture. After several seconds, the wind turbine reached a new stable operating point. The pitch angle was increased to a quite high value to shed the excessive wind power at the wind speed of 15 m/s. In this case, the operation mode of the wind turbine was altered from the optimal speed tracking to rated power generation. The overshoot in captured power is accounted for by the fact that the

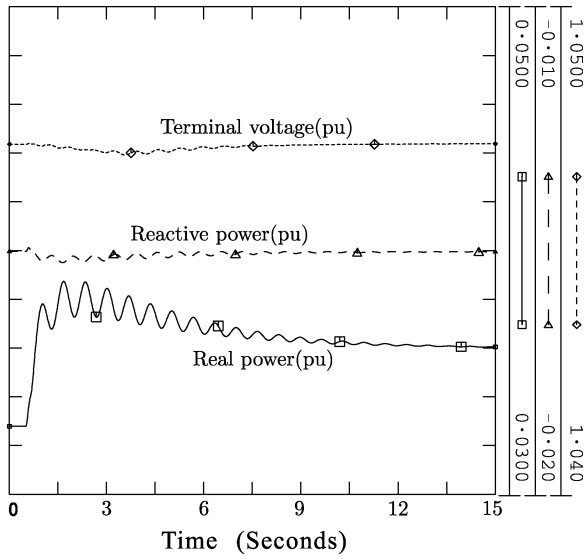

Fig. 6. Wind turbine terminal voltage and power output.

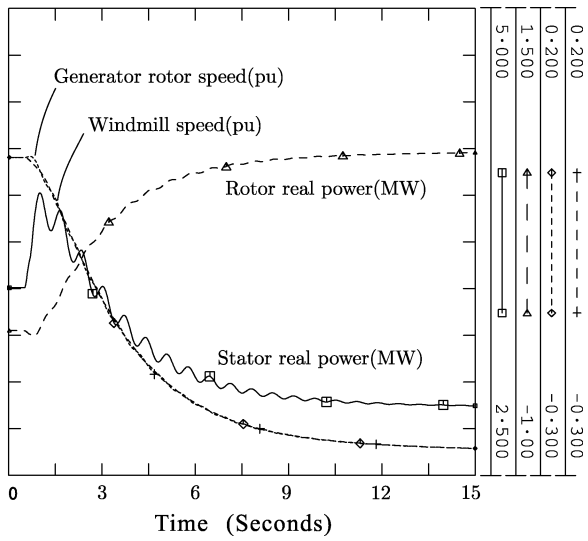

Fig. 7. Wind turbine mechanical power and speed tracking.

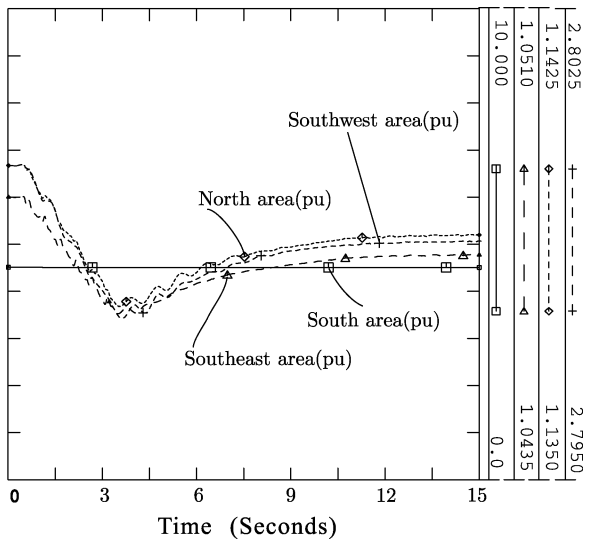

Fig. 8. Power fluctuations of representative conventional generators.

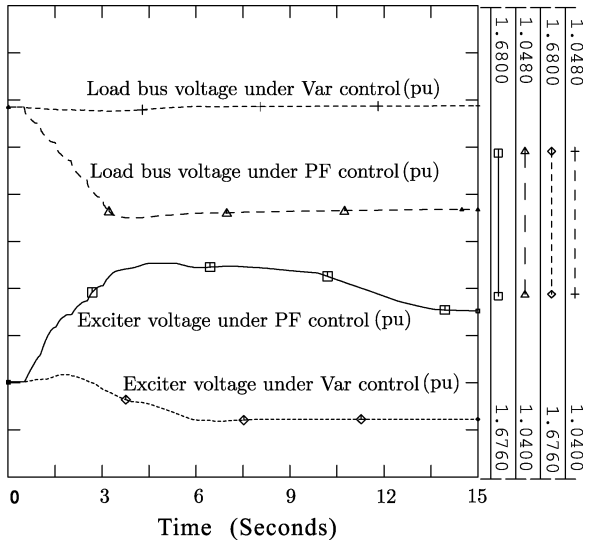

Fig. 9. Load bus and generator exciter voltage under different controls.

pitch controller cannot react instantaneously to a change in the wind speed.

As can be seen from Fig. 6, the independent control of the real power and reactive power was achieved via the vector control technique. With the wind speed increasing, the wind turbine produced more real power. Over the same period, the reactive power was kept almost constant, which minimized the impact of wind generation fluctuation on the terminal voltage profile. From Fig. 7, it can be observed that the windmill speed and rotor speed changed smoothly. The stator power decreased and the rotor power increased to accommodate the changing shaft speed. During this process, the operating state of the wind turbine changed steplessly from subsynchronous to super-synchronous as expected. The simulation in [14] also confirmed the similar change in the power flow through the stator and rotor, caused by a step change in the wind speed.

To reveal the wind park influence on the main network, responses of other power plants to the wind park fluctuation were also simulated. For simplification, four representative generators located respectively in the north, south, southwest, and southeast areas were selected. The power outputs from these generators are shown in Fig. 8. It can be seen that the wind power has the least impact on the generator located in the south area, which is far away in terms of electrical distance from the wind park site. Similar results were also observed in the exciter responses for these synchronous generators.

In the above simulations, constant Var flow has been set as the goal of wind turbine reactive power control. As a comparison, an alternative control strategy—keeping the wind turbine power factor constant, was also studied. As shown in Fig. 9, these two control policies displayed quite different impacts on nearby loads and conventional generators. In the case of Var control, the wind power fluctuation caused little disturbance on the load bus voltage and the exciter voltage of conventional generator. In the case of power-factor control, the reactive power absorbed by the wind turbine increased as did the real power,

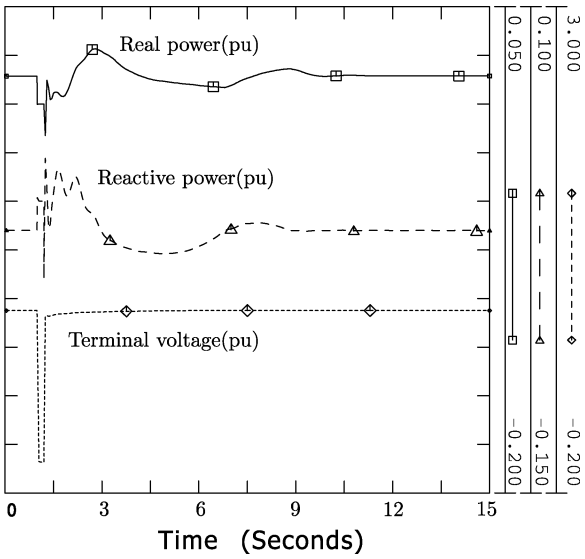

Fig. 10. Wind turbine power and voltage against electrical fault.

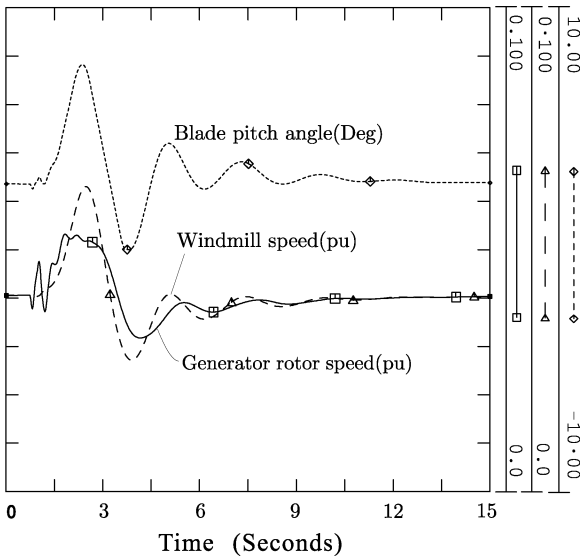

Fig. 11. Wind turbine shafts twist and pitch angle against electrical fault.

which imposed a greater disturbance on nearby loads and generators.

To test the wind turbine capability of riding through severe disturbances, a three phase bus fault lasting 200 ms close to the wind farm was simulated. In this case, the fault caused a voltage depression of about 90% and the voltage protection was set to avoid the disconnection of the wind turbine. During the fault, a crow bar was inserted into the rotor circuit to bypass the power converter when detecting an over current. The wind turbine's performance in this circumstance was shown in Fig. 10. The real and reactive power were almost zero during the fault. Once the fault was cleared and the voltage recovered, the generator began to restore and reach its pre-fault state in about 5 s. It should be noted that in the first few milliseconds after the fault clearing, the generator operated in a motoring state and absorbed a large amount of real and reactive power from the network. This phenomenon is similar to that revealed in [15, Sec. 4.2]. Over the same period, the wind turbine shaft twisted before reaching a new stable point, and the pitch controller tried to regulate the pitch angle responding to the change of power output. Fig. 11 shows the oscillation in the wind turbine shaft and pitch angle. For some severe disturbances unstable shaft oscillations may result. This phenomenon and the necessity of inclusion of a two mass shaft model for stability studies was discussed in detail in [2]. GE also pointed out that the issue was not covered by their present model however, the further investigation on the two mass shaft model was planned [20].

V. Conclusions

This paper first reviewed the electrical equations of the induction machine in the case where the rotor voltage is not equal to zero. By eliminating the flux linkage variables in these equations, a DFIG model which is compatible with transient analysis programs has been obtained. Using this model, the independent control of torque and reactive power for wind turbines was simulated in a simple way, based on the assumption that the frequency converter is ideal and simulated as a controllable voltage source. By incorporating this with the windmill aerodynamics and the pitch control, a complete DFIG equipped variable speed wind turbine model was obtained. To test the performance of the proposed model, wind turbine responses both to a step increase in wind speed and to a voltage dip caused by an electrical fault were simulated using PSS/E and compared with detailed models developed by others. In both cases, the proposed model gave valuable insight into the performance of the variable speed wind turbine equipped with a DFIG and the interaction between the wind park and the main system. As a normal dynamic simulation time step can be adopted, this model is computationally efficient and suitable for large scale power system analysis. However, due to the assumption adopted, the model cannot be used to study the internal dynamics of the power converter.

The Irish National Grid network topology and load flow forecast data can be found [Online] at http://www.eirgrid.com.

Acknowledgment

The author would like to thank Mr Nigel Crowe and Mr Herman Busschots from GE Wind Energy for providing the technical documents on GE wind turbines.

References

[1] Z. Chen and E Spooner, "Grid power quality with variable speed wind turbines," *IEEE Trans. Energy Convers.*, vol. 16, no. 2, pp. 148–153, Apr. 2001.

[2] V. Akhmatov, "Analysis of Dynamic Behavior of Electric Power Systems With Large Amount of Wind Power," Ph.D. thesis, Technical Univ. Denmark, Lyngby, Denmark, Apr. 2003.

[3] J. Rodriguez, J. L. Fernandez, and D. Beato, "Incidence on power system dynamics of high penetration of fixed speed and doubly fed wind energy systems: study of the spanish case," *IEEE Trans. Power Syst.*, vol. 17, no. 4, pp. 1089–1095, Nov. 2002.

[4] M. Machmoum, R. L. Doeuff, and F. M. Sargos, "Steay state analysis of a doubly fed asynchrounous machine supplied by a current controlled cycloconverter in the rotor," *Proc. Inst. Elect. Eng. B*, vol. 139, no. 2, pp. 114–122, 1992.

[5] P. G. Holmes and N. A. Elsonbaty, "Cycloconverter excited divided winding doubly fed machine as a wind power converter," *Proc. Inst. Elect. Eng. B*, vol. 131, no. 2, pp. 61–69, 1984.

[6] P. W. Carlin, A. X. Laxson, and E. B. Muljadi, "The History and State of the Art of Variable-Speed Wind Turbine Technology," National Renewable Energy Lab., Tech. Rep. NREL/TP-500-28 607, Feb. 2001.
[7] A. Neris, N. Vovos, and G. Giannakopaulos, "A variable speed wind energy conversion scheme for connection to weak ac systems," *IEEE Trans. Energy Convers.*, vol. 14, no. 1, pp. 122–127, Mar. 1999.
[8] S. Doradla, S. Chakrovorty, and K. Hole, "A new slip power recovery scheme with improved supply power factor," *IEEE Trans. Power Electron.*, vol. PE-3, no. 2, pp. 200–207, Apr. 1988.
[9] R. Pena, J. Clare, and G. Asher, "Doubly fed induction generator using back-to-back pwm converters and its application to variable-speed wind-energy generation," *Proc. Inst. Elect. Eng., Electric Power Applications*, vol. 143, no. 3, pp. 231–241, May 1996.
[10] L. Refoufi, B. A. Zahawi, and A. Jack, "Analysis and modeling of the steady state behavior of the static kramer induction generator," *IEEE Trans. Energy Convers.*, vol. 14, no. 3, pp. 333–339, Sep. 1999.
[11] L. Xu and W. Cheng, "Torque and reactive power control of a doubly fed induction machine by position sensorless scheme," *IEEE Trans. Ind. Appl.*, vol. 31, no. 3, pp. 636–642, May/Jun. 1995.
[12] I. Cadirci and M. Ermis, "Double-output induction generator operating at subsynchronous and supersynchronous speeds: steady-state performance optimization and wind-energy recovery," *Proc. Inst. Elect. Eng., Electric Power Applications*, vol. 139, no. 5, pp. 429–442, Sept. 1992.
[13] Y. Tang and L. Xu, "A flexible active and reactive power control strategy for a variable speed constant frequency generating system," *IEEE Trans. Power Electron.*, vol. 10, no. 4, pp. 472–478, Jul. 1995.
[14] A. D. Hansen, C. Jauch, and P. Sorensen, "Dynamic Wind Turbine Models in Power System Simulation Tool Digsilent," Risø National Laboratory, Risø, Denmark, Tech. Rep. Risø-R-400(EN), Dec. 2003.
[15] "Dynamic Modeling of Doubly-Fed Induction Machine Wind-Generators," DIgSILENT GmbH, Germany, Tech. Rep., Aug. 2003.
[16] A. Feijo, J. Cidrs, and C. Carrillo, "Third order model for the doubly-fed induction machine," *Elect. Power Syst. Res.*, vol. 56, pp. 121–127, Mar. 2000.
[17] P. Kundur, *Power System Stability and Control*. New York: McGraw-Hill, 1994.
[18] L. Tang and R. Zavadil, "Shunt capacitor failures due to windfarm induction generator self-excitation phenomenon," *IEEE Trans. Energy Convers.*, vol. 8, no. 3, pp. 513–519, Sep. 1993.
[19] M. M. Hand and M. J. Balas, "Systematic Controller Design Methodology for Variable-Speed Wind Turbines," National Renewable Energy Laboratory, Tech. Rep. NREL/TP-500-29 415, Feb. 2002.
[20] N. W. Miller, J. J. Sanchez-Gasca, and W. W. Price, "Dynamic modeling of GE 1.5 and 3.6 MW wind turbine generators for stability simulations," in *Proc. IEEE Power Engineering Society General Meeting*, vol. 3, Jul. 2003, pp. 1977–1983.

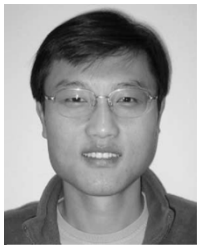

Yazhou Lei was born in Liaoning, China, in 1973. He received the B.Eng. and M.Eng. degrees from Northeast China Electric Power Institute in 1995 and 1998, respectively, and the Ph.D. degree from China Electric Power Research Institute in 2001, all in electrical power system engineering.

In 2002, he began postdoctoral research on the modeling and control of wind turbines at the Department of Electrical and Electronic Engineering, University College Cork, Cork, Ireland. Prior to that, he was with the Power System Group at China Electric Power Research Institute. His primary fields of interest are power system stability/control and wind power generation.

Alan Mullane received the B.E. degree in 1998 and the Ph.D. degree in the area of modeling and control of wind energy conversion systems in 2003, both from University College Cork, Cork, Ireland.

He is currently a postdoctoral Research Fellow with the Energy Research Center at University College Dublin (UCD), funded by Sustainable Energy Ireland (SEI) and is acting as the national representative for the IEA Wind Annex XXI: dynamic models of wind farms for power system studies.

Gordon Lightbody received the M.Eng. degree (with distinction) in 1989 and the Ph.D. degree in electrical and electronic engineering in 1993, both from Queen University Belfast (QUB), Belfast, U.K.

His research interests include nonparametric modeling, local model networks for process modeling and control, model-based predictive control, fuzzy/neural systems, and nonlinear control. This work is focused on key application areas, including wind power, power system control and harmonic analysis. He has published over 60 papers

Dr. Lightbody has received prizes at the ACC 1995 in Seattle, WA, the Institute of Electrical Engineers (IEE) Control 1994 in Warwick, U.K., and an honorable mention at the IFAC World Congress in San Francisco, 1996. He was a member of the Applied Control Techniques committee (C9) of the IEE (1996–1997), the new Intelligent Control Committee (B4) of the IEE (1997–2000), and part of the management team to the new IEE Professional Network on Concepts for Automation and Control. He is also an Associate Editor for the IFAC journal *Control Engineering Practice*.

Robert Yacamini is a Professor of electrical engineering at University College Cork, Cork, Ireland.